JOURNAL OF MOLECULAR SPECTROSCOPY 94, 100–113 (1982)

Direct Observation of the ν_1 and ν_3 Fundamental Bands of NH_2 by Difference Frequency Laser Spectroscopy

T. AMANO, P. F. BERNATH, AND A. R. W. MCKELLAR

Herzberg Institute of Astrophysics, National Research Council of Canada, Ottawa, Ontario K1A 0R6, Canada

The ν_1 and ν_3 bands of the NH_2 radical were detected in absorption in the 2.9- to 3.2-μm region using a tunable difference frequency laser and a long-path Zeeman-modulated discharge cell. About 100 rotation–vibration transitions were measured and a simultaneous analysis of the Coriolis-coupled ν_1 and ν_3 states was made. It was found that the ν_1 band is considerably stronger than ν_3, in contrast to the similar molecule H_2O. These results may prove useful in a search for interstellar NH_2 by means of its rotation–vibration spectrum.

I. INTRODUCTION

The NH_2 radical has been the subject of extensive high-resolution spectroscopic analysis, particularly by means of its $\tilde{A}^2A_1$–$\tilde{X}^2B_1$ electronic transition in the visible region (*1–6*), but studies of its infrared spectrum have been relatively limited. In 1965 two features were observed by Milligan and Jacox (*7*) in the low-temperature matrix isolation spectrum of photolyzed NH_3 at 1499 and 3220 cm^{-1}, which were assigned by them as the ν_2 (bend) and ν_3 (asymmetric stretch) vibrations, respectively, of NH_2. Recently, the ν_2 band in the gas phase has been observed and analyzed using laser magnetic resonance spectroscopy (*8*). In addition to direct infrared observations, information on the excited vibrational states of NH_2 also has been obtained from the electronic spectrum. Kroll (*4*) obtained a vibrational frequency of 3221 cm^{-1} from an analysis of laser-induced fluorescence data and concluded that it was the ν_1 (symmetric stretch) vibration rather than ν_3, because of the observed selection rules. By detailed analyses of the visible emission spectrum, Birss *et al.* (*5*) have studied the $(v_1v_2v_3) = (020)$ excited bending state and very recently Vervloet and Merienne-Lafore (*6*) have obtained an improved value of $\nu_1 = 3219.36$ cm^{-1} and a tentative value of $\nu_3 = 3280$ cm^{-1}. Their detection of levels in the $v_3 = 1$ state was made possible by Coriolis perturbations between the (100) and (001) states.

In the present paper, we report the direct detection of the ν_1 and ν_3 fundamental bands of NH_2 in the 2.9- and 3.2-μm region of the infrared. About 100 rotation–vibration transitions have been measured and a detailed analysis of the Coriolis-coupled (100) and (001) states has been made. Our results confirm, and considerably extend, those of Vervloet and Merienne-Lafore (*6*). The observations were made using a tunable difference frequency laser system and a long pathlength Zeeman-modulated discharge absorption cell. The difference frequency laser was developed as a high-resolution spectroscopic tool by Pine (*9*). Our laser system was

0022-2852/82/070100-14$02.00/0

constructed by Oka (*10*) for use in studying unstable molecules and the detection of the spectrum of H_3^+ by Oka (*11*) confirmed the value of the technique for such transient species. Vibrational spectra of two further ions, HeH^+ (*12*) and NeH^+ (*13*), have since been studied using Oka's original apparatus. By adding Zeeman modulation to an absorption cell similar to that used for these ions, a number of paramagnetic free radicals have been detected in the 3-μm region, of which NH_2 was the first. Similar studies of free radicals have been made in other laboratories using tunable infrared diode lasers (*14*) and color center lasers (*15*).

II. EXPERIMENTAL DETAILS

The apparatus used in this investigation is shown schematically in Fig. 1. The difference frequency laser system was almost identical to that of Oka (*10*, *11*). Visible radiation from a cw single-mode tunable dye laser is mixed with that from a single-mode Ar^+ laser in a temperature-controlled lithium niobate crystal. The resulting difference frequency lies in the infrared and may be tuned over a range of about 2.2 to 4.4 μm with a power of a few microwatts. The infrared linewidth is governed by those of the two visible lasers and was of the order of 10 MHz.

The discharge absorption cell used here was similar to that used by Oka for H_3^+ (*11*) with the addition of provision for Zeeman modulation. It was made from a 2.4-cm-diam. pyrex tube fitted with cylindrical electrodes and Brewster angle end windows. Multiple-reflection mirrors were located outside the cell adjacent to the cell windows and the cell was wrapped with a two layer solenoidal modulation coil with about 8.5 turns/cm. The modulated field length was 1 m, the discharge length

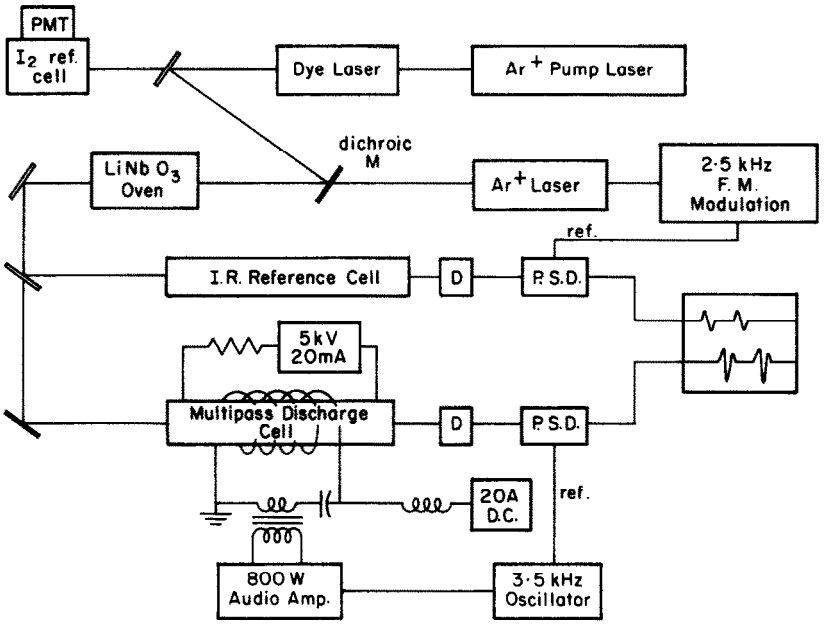

FIG. 1. Schematic diagram of the apparatus used in this investigation.

1.5 m, and the mirror separation 2 m. A sinusoidal modulation current at 3.5 kHz was applied to the coil along with a variable dc bias to achieve zero-based field modulation. The maximum current of about 20 A gave a modulation amplitude of about 200 G (peak to peak). The modulation current, from a high-power audio amplifier, and the bias current were matched to the Zeeman coil with a transformer and tuned LC series circuit as shown in Fig. 1. The cell and coil were cooled by immersion in either ice or dry ice baths.

The infrared laser beam was passed through the cell 16 times for a total effective modulated path of about 16 m. Part of the infrared beam was directed through a reference gas cell for wavelength calibration purposes (see Fig. 1) and each infrared beam was monitored by a liquid nitrogen cooled InSb detector. In addition to the Zeeman modulation, we also employed simultaneous frequency modulation of the infrared radiation at 2.5 kHz in order to record the reference gas spectrum. The spectra of C_2H_4 (*16*) and N_2O (*17*) were used for reference and the accuracy of the NH_2 measurements is estimated to be about 0.003 cm^{-1}.

NH_2 was produced by a dc discharge in flowing NH_3 at a pressure of about 0.8 Torr and a discharge current of about 30 mA. Before searching for the infrared spectrum, we monitored the visible laser-induced fluorescence from NH_2; this observation, and the infrared study, showed that the NH_2 production was not critically dependent on the pressure, current or pumping speed.

III. RESULTS AND ANALYSIS

The term values obtained by Vervloet and Merienne-Lafore (*6*) for the $v_1 = 1$ state were used to predict transition frequencies for our initial searches. After a number of ν_1 band lines were found, some strongly perturbed ν_3 band lines were also detected on the basis of Ref. (*6*). Analysis of these preliminary infrared measurements resulted in more accurate and extensive predictions for both bands and ultimately 59 rotation–vibration transitions were identified in ν_1 and 37 in ν_3; the measurements are listed, together with their assignments, in Tables I and II. For each such transition we generally measured two or more fine-structure components.

Examples of ν_1 and ν_3 band transitions detected using the Zeeman-modulation technique are shown in Figs. 2 and 3, respectively. The ν_1 band transitions were generally much stronger than those of ν_3 as is discussed in more detail below. A more detailed look at one part of the absorption spectrum of discharged ammonia is shown in Fig. 4. The upper trace in Fig. 4 is a conventional transmission spectrum recorded by chopping the infrared beam followed by phase-sensitive detection. Two prominent NH_3 lines are evident in this trace. Much greater sensitivity is gained by using frequency modulation as shown in the two middle traces of Fig. 4. With the discharge on, new lines appear in the spectrum, some of which are probably due to hot NH_3. However, three of these new features are due to NH_2, as shown by the lowest trace, which was taken using Zeeman modulation. The region of Fig. 4 is relatively free of NH_3 absorption compared to much of the spectrum that we surveyed and Zeeman modulation was useful for identification but not essential for detection. However, in many other regions the Zeeman modulation was essential for the detection of the NH_2 transitions.

TABLE I

Observed Transitions in the ν_1 Fundamental Band of NH_2

Assignment										Observed	O - C
$N_{K_aK_c}$						J				(cm^{-1})	(cm^{-1})
6	0	6	←	6	1	5	5.5	←	5.5	3126.211	0.000
6	0	6	←	6	1	5	6.5	←	6.5	3126.373	-0.002
4	3	1	←	4	4	0	3.5	←	3.5	3126.147	-0.006[a]
4	3	1	←	4	4	0	4.5	←	4.5	3126.600	0.001[a]
1	1	1	←	2	2	0	1.5	←	1.5	3133.233	0.002
1	1	1	←	2	2	0	0.5	←	1.5	3133.453	-0.000
1	1	1	←	2	2	0	1.5	←	2.5	3133.757	-0.001
1	1	0	←	2	2	1	0.5	←	1.5	3139.495	0.002
1	1	0	←	2	2	1	1.5	←	2.5	3139.767	0.001
4	2	3	←	4	3	2	3.5	←	3.5	3145.803	0.007
4	2	3	←	4	3	2	4.5	←	4.5	3146.122	0.007
3	1	3	←	4	0	4	3.5	←	4.5	3146.035	0.002
3	1	3	←	4	0	4	2.5	←	3.5	3146.057	-0.001
3	2	2	←	3	3	1	2.5	←	2.5	3150.293	-0.002
3	2	2	←	3	3	1	3.5	←	3.5	3150.696	-0.001
2	0	2	←	3	1	3	2.5	←	2.5	3155.519	-0.000
2	0	2	←	3	1	3	1.5	←	2.5	3155.577	0.001
2	0	2	←	3	1	3	2.5	←	3.5	3155.647	0.005
4	2	2	←	4	3	1	3.5	←	3.5	3158.894	0.005
4	2	2	←	4	3	1	4.5	←	4.5	3159.243	0.009
3	1	3	←	3	2	2	2.5	←	2.5	3162.637	0.002
3	1	3	←	3	2	2	3.5	←	3.5	3162.925	-0.000
1	0	1	←	2	1	2	0.5	←	1.5	3170.765	0.002
1	0	1	←	2	1	2	1.5	←	2.5	3170.880	0.004
2	1	2	←	2	2	1	1.5	←	1.5	3171.466	-0.004
2	1	2	←	2	2	1	2.5	←	2.5	3171.854	-0.002
4	1	3	←	4	2	2	3.5	←	3.5	3181.445	-0.003
4	1	3	←	4	2	2	4.5	←	4.5	3181.590	-0.004
2	1	1	←	2	2	0	2.5	←	1.5	3184.259	-0.000
2	1	1	←	2	2	0	1.5	←	1.5	3184.459	0.002
2	1	1	←	2	2	0	2.5	←	2.5	3184.786	-0.000
3	0	3	←	3	1	2	2.5	←	2.5	3184.864	0.000
3	0	3	←	3	1	2	3.5	←	3.5	3184.990	0.003
3	1	2	←	3	2	1	2.5	←	2.5	3185.020	0.003
3	1	2	←	3	2	1	3.5	←	3.5	3185.235	0.006
0	0	0	←	1	1	1	0.5	←	0.5	3187.366	0.001
0	0	0	←	1	1	1	0.5	←	1.5	3187.598	0.002
1	1	1	←	2	0	2	1.5	←	1.5	3188.328	-0.000
1	1	1	←	2	0	2	1.5	←	2.5	3188.386	0.001
1	1	1	←	2	0	2	0.5	←	1.5	3188.546	-0.005
2	0	2	←	2	1	1	2.5	←	1.5	3196.633	0.003
2	0	2	←	2	1	1	1.5	←	1.5	3196.688	0.001
2	0	2	←	2	1	1	2.5	←	2.5	3196.831	-0.003
2	0	2	←	2	1	1	1.5	←	2.5	3196.889	-0.002
1	0	1	←	1	1	0	1.5	←	0.5	3203.343	0.004
1	0	1	←	1	1	0	0.5	←	0.5	3203.376	0.002
1	0	1	←	1	1	0	1.5	←	1.5	3203.605	0.000
1	0	1	←	1	1	0	0.5	←	1.5	3203.638	-0.001
2	2	0	←	3	1	3	2.5	←	3.5	3208.760	-0.000
2	2	0	←	3	1	3	1.5	←	2.5	3209.146	0.000
1	1	0	←	1	0	1	1.5	←	0.5	3234.018	-0.005
1	1	0	←	1	0	1	1.5	←	1.5	3234.052	-0.004
1	1	0	←	1	0	1	0.5	←	0.5	3234.276	-0.002

[a] These less accurately measured transitions were given reduced weight (0.1) in the least-squares fit.

[b] These uncertain measurements were omitted from the least-squares fit.

The lineshapes exhibited by the Zeeman-modulated traces in Figs. 2–4 are functions of the modulation amplitude and the spin-splittings of the energy levels involved in each transition. Identification of the true line center was usually fairly

TABLE I—*Continued*

Assignment									Observed	O - C
$N_{K_aK_c}$						J			(cm^{-1})	(cm^{-1})
1	1	0	←	1	0	1	0.5	← 1.5	3234.309	-0.003
2	1	1	←	2	0	2	2.5	← 1.5	3239.358	0.001
2	1	1	←	2	0	2	2.5	← 2.5	3239.415	0.001
2	1	1	←	2	0	2	1.5	← 1.5	3239.553	-0.002
2	1	1	←	2	0	2	1.5	← 2.5	3239.611	-0.001
3	2	1	←	3	1	2	3.5	← 3.5	3247.400	-0.001
3	2	1	←	3	1	2	2.5	← 2.5	3247.592	-0.001
4	2	2	←	4	1	3	4.5	← 4.5	3247.658	0.008
4	2	2	←	4	1	3	3.5	← 3.5	3247.764	0.007
3	1	2	←	3	0	3	3.5	← 2.5	3249.016	-0.004
3	1	2	←	3	0	3	3.5	← 3.5	3249.095	-0.005
3	1	2	←	3	0	3	2.5	← 2.5	3249.217	-0.001
3	1	2	←	3	0	3	2.5	← 3.5	3249.296	-0.002
2	2	0	←	2	1	1	2.5	← 1.5	3249.746	-0.002
2	2	0	←	2	1	1	2.5	← 2.5	3249.950	-0.002
2	2	0	←	2	1	1	1.5	← 1.5	3250.257	0.001
2	2	0	←	2	1	1	1.5	← 2.5	3250.462	0.002
1	1	1	←	0	0	0	1.5	← 0.5	3250.429	0.000
1	1	1	←	0	0	0	0.5	← 0.5	3250.656	0.005
5	2	3	←	5	1	4	5.5	← 5.5	3254.031	-0.004
5	2	3	←	5	1	4	4.5	← 4.5	3254.130	-0.001
2	2	1	←	2	1	2	2.5	← 2.5	3262.939	-0.001
2	2	1	←	2	1	2	1.5	← 1.5	3263.301	-0.001
4	1	3	←	4	0	4	4.5	← 4.5	3263.141	0.000
4	1	3	←	4	0	4	3.5	← 3.5	3263.263	-0.000
2	1	2	←	1	0	1	2.5	← 1.5	3266.148	0.002
2	1	2	←	1	0	1	1.5	← 0.5	3266.254	-0.001
2	1	2	←	1	0	1	1.5	← 1.5	3266.290	0.001
4	3	1	←	4	2	2	4.5	← 4.5	3266.747	-0.000
4	3	1	←	4	2	2	3.5	← 3.5	3267.014	-0.002
3	0	3	←	2	1	2	2.5	← 1.5	3268.655	-0.002
3	0	3	←	2	1	2	3.5	← 2.5	3268.727	0.002
3	0	3	←	2	1	2	2.5	← 2.5	3268.805	0.001
3	2	2	←	3	1	3	3.5	← 3.5	3269.816	-0.005
3	2	2	←	3	1	3	2.5	← 2.5	3270.096	0.001
3	3	0	←	3	2	1	3.5	← 3.5	3273.254	0.005
3	3	0	←	3	2	1	2.5	← 2.5	3273.620	0.001
3	3	1	←	3	2	2	3.5	← 3.5	3278.922	0.002
3	3	1	←	3	2	2	2.5	← 2.5	3279.295	0.001
4	2	3	←	4	1	4	4.5	← 4.5	3278.963	0.003
4	2	3	←	4	1	4	3.5	← 3.5	3279.203	0.009[a]
3	1	3	←	2	0	2	3.5	← 2.5	3279.674	-0.003
3	1	3	←	2	0	2	2.5	← 1.5	3279.740	0.000
3	1	3	←	2	0	2	2.5	← 2.5	3279.790	-0.007[b]
4	1	3	←	3	2	2	3.5	← 2.5	3279.835	-0.004
4	1	3	←	3	2	2	4.5	← 3.5	3280.029	-0.004
4	3	2	←	4	2	3	4.5	← 4.5	3280.695	-0.001
4	3	2	←	4	2	3	3.5	← 3.5	3280.982	-0.003
5	3	3	←	5	2	4	5.5	← 5.5	3284.445	-0.002
5	3	3	←	5	2	4	4.5	← 4.5	3284.682	-0.003
4	0	4	←	3	1	3	3.5	← 2.5	3286.736	-0.005
4	0	4	←	3	1	3	4.5	← 3.5	3286.767	-0.002
5	2	4	←	5	1	5	5.5	← 5.5	3290.054	0.055[b]

clear but uncertainties in doing this sometimes contributed errors of the same magnitude ($\sim$0.003 cm^{-1}) as our absolute measurement accuracy.

The net electron spin, $S = 1/2$, of NH_2 in its $^2B_1$ ground electronic state results in a splitting of each rotational energy level, denoted by N_{KaKc}, into two components. The resulting angular momentum is $\mathbf{J} = \mathbf{N} + \mathbf{S}$, and in NH_2 the level with $J = N - 1/2$ ("F_2") is located above the level with $J = N + 1/2$ ("F_1"). Our analysis was carried out using a doublet asymmetric rotor computer program originally developed to analyze laser magnetic resonance spectra of Coriolis-coupled bands

TABLE I—*Continued*

Assignment										Observed	O - C
$N_{K_aK_c}$						J				(cm^{-1})	(cm^{-1})
5	2	4	←	5	1	5	4.5	←	4.5	3290.276	0.063[b]
4	1	4	←	3	0	3	4.5	←	3.5	3292.469	-0.001
4	1	4	←	3	0	3	3.5	←	2.5	3292.504	0.001
5	4	1	←	5	3	2	5.5	←	5.5	3293.567	0.001
5	4	1	←	5	3	2	4.5	←	4.5	3293.825	0.006
2	2	1	←	1	1	0	2.5	←	1.5	3295.665	-0.003
2	2	1	←	1	1	0	1.5	←	0.5	3295.912	-0.001
2	2	1	←	1	1	0	1.5	←	1.5	3296.177	-0.001
6	1	5	←	6	0	6	6.5	←	6.5	3296.741	-0.001
6	1	5	←	6	0	6	5.5	←	5.5	3296.909	0.005
4	4	0	←	4	3	1	4.5	←	4.5	3297.177	-0.009[a]
4	4	0	←	4	3	1	3.5	←	3.5	3297.519	-0.002
4	4	1	←	4	3	2	4.5	←	4.5	3298.886	-0.005
4	4	1	←	4	3	2	3.5	←	3.5	3299.196	-0.000
5	4	2	←	5	3	3	5.5	←	5.5	3300.555	-0.001
5	4	2	←	5	3	3	4.5	←	4.5	3300.698	0.007
2	2	0	←	1	1	1	2.5	←	1.5	3301.712	-0.002
2	2	0	←	1	1	1	1.5	←	0.5	3301.991	0.000
2	2	0	←	1	1	1	1.5	←	1.5	3302.222	0.000
5	0	5	←	4	1	4	4.5	←	3.5	3302.954	-0.004
5	0	5	←	4	1	4	5.5	←	4.5	3302.966	-0.002
5	1	5	←	4	0	4	5.5	←	4.5	3305.562	0.006
5	1	5	←	4	0	4	4.5	←	3.5	3305.582	0.009
3	3	1	←	2	2	0	3.5	←	2.5	3341.046	0.002
3	3	1	←	2	2	0	2.5	←	1.5	3341.305	0.003
3	3	0	←	2	2	1	3.5	←	2.5	3342.468	0.004
3	3	0	←	2	2	1	2.5	←	1.5	3342.718	0.002
4	3	2	←	3	2	1	4.5	←	3.5	3358.247	-0.001
4	3	2	←	3	2	1	3.5	←	2.5	3358.484	-0.002
4	3	1	←	3	2	2	4.5	←	3.5	3365.186	-0.000
4	3	1	←	3	2	2	3.5	←	2.5	3365.405	-0.002
5	3	3	←	4	2	2	5.5	←	4.5	3371.884	-0.001
5	3	3	←	4	2	2	4.5	←	3.5	3372.089	-0.004

(*18*). The *A*-reduced asymmetric rotor Hamiltonian of Watson (*19*) was used together with the spin–rotation Hamiltonian of Brown and Sears (*20*) (see, for example, Eqs. (1) and (2) of (*21*)). It was necessary to analyze the ν_1 and ν_3 band data simultaneously because of the *c*-type Coriolis interaction between the (100) and (001) states. This interaction gives rise to an additional term in the rotational Hamiltonian connecting the two states given by

$$H_{\text{cor}} = i\xi^c_{13}N_c + Z(N_aN_b + N_bN_a). \tag{1}$$

The resulting matrix elements are given by

$$\langle v, J, N, k|H_{\text{cor}}|v', J, N, k \pm 1\rangle = [\pm(1/2)\xi^c_{13} + Z(k \pm 1/2)] \times [N(N+1) - k(k \pm 1)]^{1/2}, \tag{2}$$

where v = (100) and v' = (001). The constant ξ is related to the usual Coriolis coupling constant ζ by

$$\xi^c_{13} = \zeta^c_{13}C[(\nu_1/\nu_3)^{1/2} + (\nu_3/\nu_1)^{1/2}], \tag{3}$$

and Z is a higher-order term which is essentially a K-dependent correction to ξ. Our Z is equivalent to h_{43} of Flaud and Camy-Peyret (*22*) and to F of Tanaka and Morino (*23*). The resulting molecular Hamiltonian was set up in a Wang-type

TABLE II

Observed Transitions in the ν_3 Fundamental Band of NH_2

Assignment												Observed	O - C
$N_{K_a}K_c$						J						(cm^{-1})	(cm^{-1})
4	1	4	←	5	1	5	4.5	←	5.5			3208.826	-0.004
4	1	4	←	5	1	5	3.5	←	4.5			3208.868	0.005
3	0	3	←	4	0	4	3.5	←	4.5			3224.571	0.004
3	0	3	←	4	0	4	2.5	←	3.5			3224.550	-0.002
3	1	3	←	4	1	4	3.5	←	4.5			3226.101	0.005
3	1	3	←	4	1	4	2.5	←	3.5			3226.101	0.001
2	2	1	←	3	2	2	2.5	←	3.5			3233.395	0.002
2	2	1	←	3	2	2	1.5	←	2.5			3233.470	0.001
4	1	4	←	4	1	3	4.5	←	4.5			3252.632	-0.002
4	1	4	←	4	1	3	3.5	←	3.5			3252.562	-0.006
1	1	0	←	2	1	1	1.5	←	2.5			3252.999	0.003
1	1	0	←	2	1	1	0.5	←	1.5			3253.039	0.001
1	0	1	←	2	0	2	1.5	←	2.5			3259.989	0.001
1	0	1	←	2	0	2	0.5	←	1.5			3259.965	-0.001
1	1	1	←	2	1	2	1.5	←	2.5			3262.470	0.001
1	1	1	←	2	1	2	0.5	←	1.5			3262.534	0.001
4	2	3	←	4	2	2	4.5	←	4.5			3280.883	-0.000
4	2	3	←	4	2	2	3.5	←	3.5			3280.869	-0.001
4	4	1	←	4	4	0	4.5	←	4.5			3284.640	-0.001
4	4	1	←	4	4	0	3.5	←	3.5			3284.554	-0.001
2	1	2	←	2	1	1	2.5	←	2.5			3285.291	0.001
2	1	2	←	2	1	1	1.5	←	1.5			3285.224	0.000
3	2	2	←	3	2	1	2.5	←	2.5			3290.590	-0.003
3	2	2	←	3	2	1	3.5	←	3.5			3290.614	-0.002
3	3	1	←	3	3	0	2.5	←	2.5			3291.390	0.002
3	3	1	←	3	3	0	3.5	←	3.5			3291.452	-0.000
3	3	0	←	3	3	1	2.5	←	2.5			3291.875	0.000
3	3	0	←	3	3	1	3.5	←	3.5			3291.932	0.000
5	3	2	←	5	3	3	5.5	←	5.5			3292.065	0.003
5	3	2	←	5	3	3	4.5	←	4.5			3292.189	-0.005
1	1	1	←	1	1	0	0.5	←	0.5			3295.139	-0.004
1	1	1	←	1	1	0	1.5	←	1.5			3295.195	-0.003
2	2	1	←	2	2	0	1.5	←	1.5			3295.475	-0.002
2	2	1	←	2	2	0	2.5	←	2.5			3295.516	-0.002
2	2	0	←	2	2	1	2.5	←	2.5			3298.179	0.003
2	2	0	←	2	2	1	1.5	←	1.5			3298.135	0.002
3	2	1	←	3	2	2	2.5	←	2.5			3302.612	0.002
3	2	1	←	3	2	2	3.5	←	3.5			3302.636	-0.001
1	1	0	←	1	1	1	0.5	←	0.5			3304.773	0.000
1	1	0	←	1	1	1	1.5	←	1.5			3304.755	-0.003
2	1	1	←	2	1	2	2.5	←	2.5			3313.947	0.002
2	1	1	←	2	1	2	1.5	←	1.5			3313.994	0.003
1	0	1	←	0	0	0	1.5	←	0.5			3322.031	-0.001
1	0	1	←	0	0	0	0.5	←	0.5			3322.068	0.002
2	1	2	←	1	1	1	2.5	←	1.5			3337.050	-0.002
2	1	2	←	1	1	1	1.5	←	1.5			3337.189	-0.001
2	0	2	←	1	0	1	1.5	←	0.5			3341.387	0.000
2	0	2	←	1	0	1	2.5	←	1.5			3341.359	-0.003
2	1	1	←	1	1	0	1.5	←	0.5			3346.599	-0.003
2	1	1	←	1	1	0	2.5	←	1.5			3346.672	-0.001
3	1	3	←	2	1	2	3.5	←	2.5			3354.391	-0.003
3	1	3	←	2	1	2	2.5	←	1.5			3354.361	-0.004
3	0	3	←	2	0	2	3.5	←	2.5			3358.212	0.002

prolate symmetric rotor basis set and the resulting matrices were numerically diagonalized to obtain the molecular energy levels as part of the fitting program (*18*).

In the least-squares fit the constants of the (000) ground vibrational state were fixed at the values obtained by Birss *et al.* (*21*). The parameters resulting from the fit are listed in Table III and the quality of the fit may be judged from the residuals in Tables I and II. The rms deviation was 0.003 cm^{-1}, which is just equal to our

TABLE II—*Continued*

Assignment												J		Observed (cm^{-1})	O - C (cm^{-1})
$N_{K_aK_c}$															
3	0	3	←	2	0	2						2.5	← 1.5	3358.238	0.004
3	2	2	←	2	2	1						3.5	← 2.5	3359.830	-0.002
3	2	2	←	2	2	1						2.5	← 1.5	3359.689	-0.001
3	2	1	←	2	2	0						3.5	← 2.5	3364.763	0.001
3	2	1	←	2	2	0						2.5	← 1.5	3364.619	0.001
3	1	2	←	2	1	1						3.5	← 2.5	3368.528	-0.008[a]
3	1	2	←	2	1	1						2.5	← 1.5	3368.528	-0.001[a]
4	1	4	←	3	1	3						4.5	← 3.5	3371.333	-0.035[b]
4	1	4	←	3	1	3						3.5	← 2.5	3371.357	-0.033[b]
4	3	2	←	3	3	1						3.5	← 2.5	3376.239	0.006[a]
4	3	2	←	3	3	1						4.5	← 3.5	3376.367	0.013[a]
4	3	1	←	3	3	0						3.5	← 2.5	3377.505	0.002[a]
4	3	1	←	3	3	0						4.5	← 3.5	3377.619	0.007[a]
4	2	3	←	3	2	2						4.5	← 3.5	3379.320	-0.002
4	2	3	←	3	2	2						3.5	← 2.5	3379.260	-0.001
4	2	2	←	3	2	1						4.5	← 3.5	3389.115	-0.007[a]
4	2	2	←	3	2	1						3.5	← 2.5	3389.053	-0.005[a]
5	3	2	←	4	3	1						5.5	← 4.5	3398.560	0.002
5	3	2	←	4	3	1						4.5	← 3.5	3398.612	-0.004

[a] These less accurately measured transitions were given reduced weight (0.1) in the least-squares fit.

[b] These uncertain measurements were omitted from the least-squares fit.

estimated experimental uncertainty. The Coriolis parameters ξ^c_{13} and Z were highly correlated in the fit (correlation coefficient = −0.999958). A fit of virtually the same quality could be obtained by fixing ξ^c_{13} equal to zero, as indeed was done by Flaud and Camy-Peyret (*22*) in their analysis of the analogous bands of H_2O, but

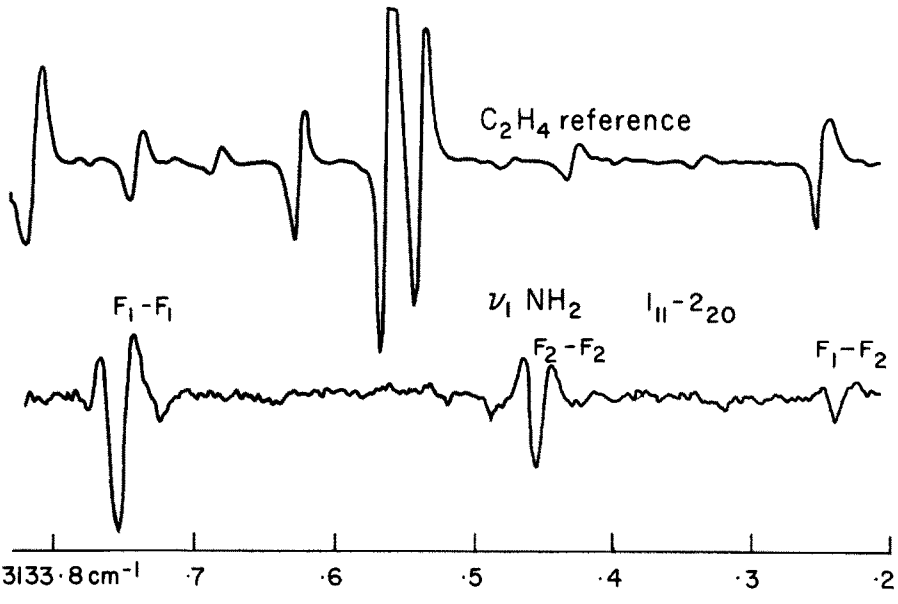

FIG. 2. The lower trace shows the $1_{11} \leftarrow 2_{20}$ transition in the ν_1 band of NH_2 recorded using the Zeeman-modulation technique. The upper trace is a spectrum of C_2H_4 for wavelength calibration recorded simultaneously using frequency modulation.

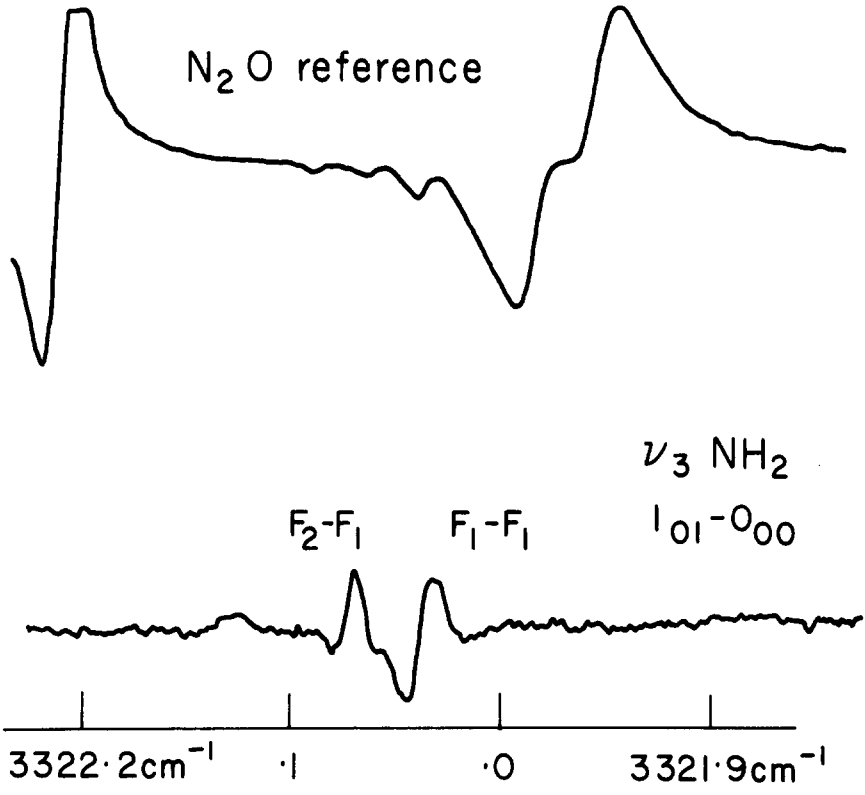

FIG. 3. The lower trace shows the $1_{01} \leftarrow 0_{00}$ transition in the ν_3 band of NH_2 recorded using Zeeman modulation. The upper trace, due to N_2O, is for wavelength calibration.

we feel that in the present case it is more realistic to allow both parameters to vary. All other correlation coefficients in the present fit had absolute values less than 0.95 and all but three were less than 0.90.

The (100) state parameters agree fairly well with those of the less precise determination by Vervloet and Merienne-Lafore (*6*). Many of the differences that do exist between the two sets of parameters may be ascribed to the fact that we explicitly included the Coriolis interaction with (001) and allowed more higher-order parameters to vary. Our value for the ν_1 band origin is just 0.01 cm^{-1} above that of (*6*). However, our value of ν_3, 3301.110 cm^{-1}, is considerably different from their estimate of 3280 cm^{-1} even though their analysis (*6*) of perturbed ν_3 state levels agrees completely with ours.

IV. DISCUSSION AND CONCLUSIONS

Except for its unpaired electron spin, the structure of NH_2 is quite similar to that of H_2O and the known ν_1 and ν_3 spectra of H_2O (*22*) provided a useful guide for the present analysis. The changes in the rotational constants of the two molecules

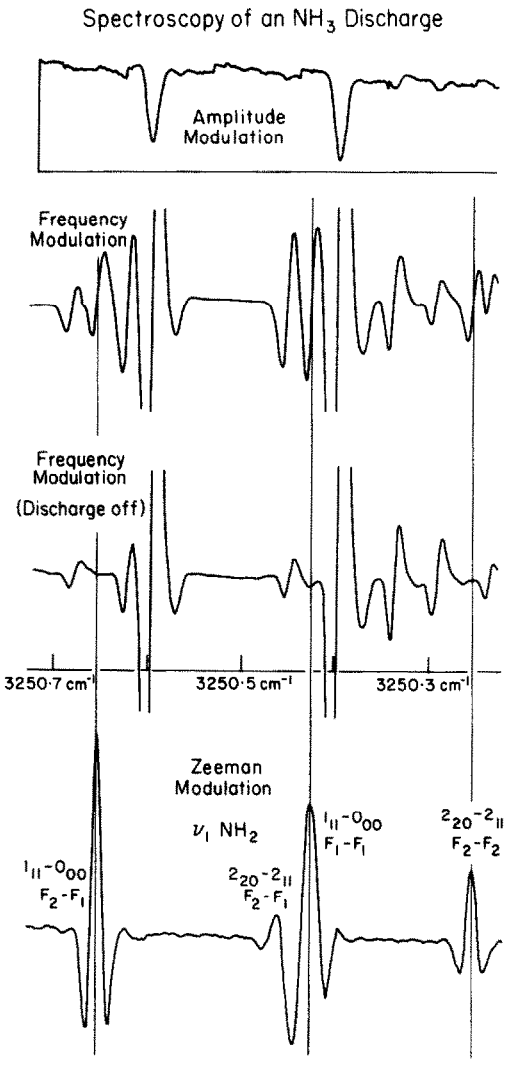

FIG. 4. A small portion of the absorption spectrum of discharged ammonia. The top trace is the conventional transmission spectrum showing two strong NH_3 lines. The two middle traces demonstrate the increase in sensitivity gained by using frequency modulation. With the discharge on a number of new lines appear in the spectrum. Three of these are due to NH_2 as is shown in the lower trace, which was taken using Zeeman modulation.

among the (000), (100), and (001) vibrational states resemble each other closely and even the values of the Coriolis parameter Z are alike ($Z = -0.303$ cm^{-1} for NH_2 and -0.319 cm^{-1} for H_2O (*22*)). One can calculate from the known force field of H_2O that the Coriolis coupling constant ζ_{13}^c is zero (*22*). A similar calculation for NH_2, using approximate force constants ($f_r = 6.2$ md/Å, $f_\theta = 0.6971$ mdÅ, $f_{r\theta} = 0.224$ md, $f_{rr} = -0.100$ md/Å) gives a value of $\zeta_{13}^c = 0.00071$ or $\xi_{13}^c = 0.012$ cm^{-1}, well within the experimental range of 0.083 ± 0.088 cm^{-1}.

TABLE III

Molecular Parameters for NH_2 (in cm^{-1})

	(000) state[a]	(100) state[b]	(001) state[b]
ν_o		3219.371(1)	3301.110(1)
A	23.69344	23.12938(79)	22.64616(82)
B	12.95194	12.76959(72)	12.87854(80)
C	8.17284	8.01584(35)	8.05815(47)
Δ_K	0.021983	0.020530(120)	0.019887(81)
$10^2\ \Delta_{NK}$	-0.41550	-0.4407(74)	-0.4054(90)
$10^2\ \Delta_N$	0.10527	0.1007(15)	0.1080(17)
$10^2\ \delta_K$	0.1002	0.0801(37)	0.1090(98)
$10^3\ \delta_N$	0.4212	0.3921(33)	0.4126(121)
$10^4\ H_K$	0.6460	0.942(61)	0.6460[c]
$10^4\ H_{KN}$	-0.113	0.326(57)	-0.113[c]
$10^6\ H_{NK}$	-0.620	-19.3(25)	-0.620[c]
$10^6\ H_N$	0.411	0.89(28)	0.411[c]
ϵ_{aa}	-0.309111	-0.29605(109)	-0.28319(166)
ϵ_{bb}	-0.045173	-0.04442(55)	-0.04540(117)
$10^3\ \epsilon_{cc}$	0.4024	-0.18(42)	-0.25(72)
$10^3\ \Delta_K^S$	0.1094	0.0599(102)	0.0963(141)
		Coriolis Parameters[d]	
ζ_{13}^c		0.083(88)	
z		-0.3031(113)	

[a] Ground state parameters from Birss et al. (21). Higher order parameters not shown here were fixed at the values of (21) for all three states. Note that the definition of the sign of Δ_K^S used here is opposite to that of (21).

[b] Present results. Uncertainties in parentheses are one standard deviation from the least squares fit, expressed in units of the last quoted digit.

[c] Parameter fixed at its ground state value.

[d] Only the relative sign of the Coriolis parameters is significant.

The analysis by Flaud and Camy-Peyret (*22*) of the ν_1 and ν_3 bands of H_2O also included the $2\nu_2$ band. There is a substantial homogeneous (Fermi-type) interaction between the (020) and (100) states in H_2O, as well as small higher-order Coriolis-type interactions between (020) and both (100) and (001). Interactions with (020) were not included in the present analysis and we did not notice any adverse effects from this omission. Similarly, no evidence of perturbations was noted in the analysis of the (020) state of NH_2 made by Birss *et al.* (*5*). One reason that the interactions with the (020) state were not apparent is that the data were limited to fairly low values of N' and K_a' (6 and 4 in the present work, and 8 and 5 in (*5*)). Furthermore, the effects of a homogeneous interaction are relatively easily absorbed into other molecular parameters (this could account for the rather large change in H_{NK} between (000) and (100) in Table III). The effect of the Fermi-type interaction

between (020) and (100) has been noted for higher N by Vervloet and Merienne-Lafore (*6*) as a shift in the 8_{08} level of (100) perturbed by 8_{26} of (020).

An interesting difference between NH_2 and H_2O is that we observed the ν_1 band to be considerably stronger than ν_3, whereas just the opposite is true for H_2O. In order to examine the relative band intensities quantitatively, we have measured the $2_{21} \leftarrow 2_{12}$ transition of ν_1 and the $1_{11} \leftarrow 2_{12}$ transition of ν_3. These lines are especially suitable because they appear close together in the spectrum, they share the same lower level and they are Zeeman modulated with about the same efficiency. From their measured intensities, we estimate the ratio of the vibrational transition moments to be about $|\mu_1/\mu_3| = 4$ for NH_2, in contrast to the known value of $|\mu_1/\mu_3| = 0.223$ for H_2O (*24*). We have no explanation for this somewhat surprising result.

Table IV lists term values for NH_2 rotational levels in the (000), (100), and (001) vibrational states calculated using the constants of Table III. Each excited state energy in Table IV is followed by a number which gives the percent mixing of its eigenfunction from the *other* vibrational state. That is, a value of 0.0 indicates negligible Coriolis mixing and 50.0 indicates complete mixing. Note, for example,

TABLE IV

Calculated Energy Levels (in cm^{-1}) for NH_2

N	KA	KC	(100) STATE F1		(100) STATE F2		(001) STATE F1		(001) STATE F2		(000) STATE F1	(000) STATE F2
0	0	0	3219.371	0.0			3301.110	0.0			0.000	
1	0	1	3240.140	0.0	3240.174	0.0	3322.032	0.0	3322.066	0.0	21.109	21.143
1	1	1	3250.429	0.0	3250.651	0.0	3331.733	0.0	3331.944	0.0	31.775	32.006
1	1	0	3255.166	0.0	3255.421	0.0	3336.533	0.0	3336.779	0.0	36.535	36.800
2	0	2	3280.371	0.0	3280.427	0.0	3362.472	0.0	3362.530	0.0	62.043	62.100
2	1	2	3287.255	0.0	3287.398	0.0	3368.826	0.1	3368.964	0.1	69.264	69.411
2	1	1	3301.457	0.0	3301.655	0.0	3383.209	0.0	3383.403	0.0	83.536	83.741
2	2	1	3332.204	0.0	3332.714	0.0	3412.188	0.0	3412.675	0.0	115.400	115.928
2	2	0	3333.489	0.1	3333.997	0.1	3413.576	0.0	3414.061	0.0	116.671	117.198
3	0	3	3337.989	0.0	3338.068	0.0	3420.254	0.0	3420.334	0.0	120.744	120.824
3	1	3	3341.720	0.0	3341.840	0.0	3423.658	0.4	3423.776	0.4	124.728	124.851
3	1	2	3369.844	0.0	3370.042	0.0	3452.073	0.0	3452.269	0.0	153.002	153.205
3	2	2	3394.549	0.1	3394.947	0.1	3475.231	1.2	3475.618	1.3	178.795	179.206
3	2	1	3400.403	0.4	3400.798	0.4	3481.432	0.6	3481.816	0.6	184.615	185.025
3	3	1	3457.715	0.6	3458.500	0.6	3535.518	0.0	3536.262	0.0	243.652	244.652
3	3	0	3457.864	1.2	3458.644	1.3	3535.784	0.0	3536.527	0.0	244.066	244.874
4	0	4	3411.497	0.0	3411.592	0.0	3493.921	0.1	3494.016	0.1	195.687	195.782
4	1	4	3413.214	0.0	3413.327	0.0	3496.096	13.6	3496.241	14.8	197.561	197.676
4	1	3	3458.828	0.0	3459.045	0.0	3541.482	0.0	3541.699	0.0	243.462	243.673
4	2	3	3476.521	0.1	3476.869	0.1	3558.117	4.1	3558.467	4.3	262.168	262.526
4	2	2	3491.112	13.6	3491.430	14.8	3573.737	0.6	3574.083	0.6	277.234	277.597
4	3	2	3542.864	0.7	3543.511	0.7	3620.205	14.5	3620.885	13.3	330.407	331.074
4	3	1	3543.981	4.1	3544.613	4.3	3621.678	20.3	3622.377	18.5	331.878	332.541
4	4	1	3629.298	20.3	3630.270	18.5	3702.023	0.0	3703.015	0.0	417.350	418.428
4	4	0	3629.065	14.5	3630.062	13.3	3702.066	0.0	3703.057	0.0	417.383	418.460
5	0	5	3500.529	0.0	3500.634	0.0	3583.197	0.1	3583.301	0.1	286.466	286.570
5	1	5	3501.243	0.0	3501.355	0.0	3583.662	0.7	3583.773	0.7	287.266	287.378
5	1	4	3566.245	0.0	3566.488	0.0	3649.123	0.0	3649.367	0.0	352.793	353.039
5	2	4	3577.265	0.1	3577.591	0.1	3660.840	24.8	3661.219	26.0	364.672	365.005
5	2	3	3606.828	0.8	3607.170	0.8	3689.550	0.5	3689.890	0.4	393.807	394.159
5	3	3	3649.119	0.6	3649.690	0.6	3726.274	21.5	3726.897	20.5	438.375	438.962
5	3	2	3652.745	24.9	3653.244	26.0	3730.437	50.9	3731.157	48.8	443.666	444.263
5	4	2	3738.931	51.0	3739.654	48.8	3809.299	2.0	3810.161	2.0	525.918	526.841
5	4	1	3737.232	21.5	3738.062	20.5	3809.656	2.1	3810.516	2.0	526.198	527.119
5	5	1	3842.060	2.0	3843.373	1.9	3910.913	0.1	3912.136	0.1	634.951	636.277
5	5	0	3842.060	2.0	3843.374	1.9	3910.920	0.1	3912.142	0.1	634.956	636.282
6	0	6	3605.205	0.0	3605.314	0.0	3688.223	0.1	3688.331	0.1	393.190	393.298
6	1	6	3605.485	0.0	3605.597	0.0	3688.410	0.2	3688.520	0.2	393.514	393.625
6	1	5	3689.931	0.0	3690.202	0.0	3772.848	0.1	3773.119	0.1	478.830	479.103
6	2	5	3695.888	0.1	3696.205	0.1	3776.734	8.8	3777.062	8.5	485.425	485.748
6	2	4	3743.482	0.3	3743.838	0.3	3827.025	0.3	3827.379	0.3	532.673	533.036
6	3	4	3775.810	0.4	3776.339	0.4	3853.391	20.6	3853.961	19.9	567.132	567.674
6	3	3	3790.982	8.9	3791.478	8.7	3873.609	17.4	3874.161	18.1	580.522	581.047
6	4	3	3860.793	17.5	3861.544	18.3	3938.276	4.2	3939.057	4.1	656.399	657.221
6	4	2	3867.161	20.7	3867.905	20.0	3938.884	4.6	3940.660	4.5	657.689	658.506
6	5	2	3970.994	4.5	3972.138	4.4	4039.838	1.2	4040.921	1.2	765.264	766.430
6	5	1	3971.000	4.2	3972.145	4.1	4039.902	1.2	4040.985	1.2	765.310	766.475

NOTE: The numbers following the energies are percent mixings with the other vibratonal state (see text).

that the 5_{42} level of (100) is virtually completely mixed with 5_{32} of (001).[1] The (100) state levels in Table IV agree well with those of Vervloet and Merienne-Lafore (*6*) derived from the electronic spectrum. Moreover, the perturbed levels of (100) and (001) identified by those authors are all confirmed by our results, including the (100) $5_{42} \leftrightarrow$ (001) 5_{32} pair mentioned above.

While recording the spectrum of NH_2, transitions belonging to the fundamental band of the NH radical were also observed; these results will be reported separately (*25*). An improved version of the laser system and Zeeman-modulation cell have since been used to study CH_3 (*26*), SH (*27*), and SO (*28*). These results, and those reported here, illustrate the utility of the difference frequency laser system combined with a Zeeman-modulated discharge cell for the study of free radicals in the infrared.

ACKNOWLEDGMENTS

We would like to thank T. Oka and A. Karabonik for the construction of the difference frequency laser system, and P. Brechignac for his help in the design and construction of the Zeeman-modulation cell. We are also grateful to M. Vervloet for communication of the results of Ref. (*6*) prior to publication and to J. W. C. Johns and M. Vervloet for their comments on the manuscript.

RECEIVED: February 2, 1982

[1] Strictly speaking, the F_1 components of these two levels should be interchanged in Table IV, since their mixing coefficients exceed 50%. However, we have adopted a more "natural" labeling that conserves a reasonable spin splitting.

REFERENCES

1. K. DRESSLER AND D. A. RAMSAY, *Philos. Trans. Roy. Soc. London Ser. A.* **251,** 553–602 (1959).
2. J. W. C. JOHNS, D. A. RAMSAY, AND S. C. ROSS, *Can. J. Phys.* **54,** 1804–1814 (1976).
3. G. W. HILLS, R. S. LOWE, J. M. COOK, AND R. F. CURL, JR., *J. Chem. Phys.* **68,** 4073–4076 (1978); G. W. HILLS, J. M. COOK, R. F. CURL, JR., AND F. K. TITTEL, *J. Chem. Phys.* **65,** 823–828 (1976).
4. M. KROLL, *J. Chem. Phys.* **63,** 319–325 (1975).
5. F. W. BIRSS, M.-F. MERIENNE-LAFORE, D. A. RAMSAY, AND M. VERVLOET, *J. Mol. Spectrosc.* **85,** 493–495 (1981).
6. M. VERVLOET AND M. F. MERIENNE-LAFORE, *Can. J. Phys.* **49,** 49–55 (1982).
7. D. E. MILLIGAN AND M. E. JACOX, *J. Chem. Phys.* **43,** 4487–4493 (1965).
8. K. KAWAGUCHI, C. YAMADA, E. HIROTA, J. M. BROWN, J. BUTTENSHAW, C. R. PARENT, AND T. J. SEARS, *J. Mol. Spectrosc.* **81,** 60–72; G. W. HILLS AND A. R. W. MCKELLAR, *J. Mol. Spectrosc.* **74,** 224–227 (1979).
9. A. S. PINE, *J. Opt. Soc. Amer.* **64,** 1683–1690 (1974); **66,** 97–108 (1976).
10. P. BERNARD AND T. OKA, *J. Mol. Spectrosc.* **75,** 181–196 (1979); A. R. W. MCKELLAR AND T. OKA, *Can. J. Phys.* **56,** 1315–1320 (1978).
11. T. OKA, *Phys. Rev. Lett.* **45,** 531–534 (1980).
12. P. BERNATH AND T. AMANO, *Phys. Rev. Lett.* **48,** 20–22 (1982).
13. M. WONG, P. BERNATH, AND T. AMANO, *J. Chem. Phys.*, in press.
14. E. HIROTA, *in* "Chemical and Biochemical Applications of Lasers" (C. B. Moore, Ed.), Vol. 5, pp. 39–93, Academic Press, New York, 1980.

15. G. LITFIN, C. R. POLLOCK, R. F. CURL, JR., AND F. K. TITTEL, *J. Chem. Phys.* **72,** 6602–6605 (1980); J. PFEIFFER, D. KIRSTEN, P. KALKERT, AND W. URBAN, *Appl. Phys. B* **26,** 173–177 (1981).
16. A. S. PINE, M.I.T. Lincoln Laboratory Report No. NSF/ASRA/DAR-78-24562 (1980).
17. C. AMIOT AND G. GUELACHVILI, *J. Mol. Spectrosc.* **59,** 171–190 (1976); C. AMIOT, *J. Mol. Spectrosc.* **59,** 191–208 (1976).
18. A. R. W. MCKELLAR, *J. Chem. Phys.* **71,** 81–88 (1979); R. S. LOWE AND A. R. W. MCKELLAR, *J. Chem. Phys.* **74,** 2686–2697 (1981).
19. J. K. G. WATSON, *in* "Vibrational Spectra and Structure" (J. R. Durig, Ed.), Vol. 6, pp. 1–89, Dekker, New York, 1977.
20. J. M. BROWN AND T. J. SEARS, *J. Mol. Spectrosc.* **75,** 111–133 (1979).
21. F. W. BIRSS, D. A. RAMSAY, S. C. ROSS, AND C. ZAULI, *J. Mol. Spectrosc.* **78,** 344–346 (1979).
22. J. M. FLAUD AND C. CAMY-PEYRET, *J. Mol. Spectrosc.* **51,** 142–150 (1974).
23. T. TANAKA AND Y. MORINO, *J. Mol. Spectrosc.* **33,** 538–551 (1970).
24. J. M. FLAUD AND C. CAMY-PEYRET, *J. Mol. Spectrosc.* **55,** 278–310 (1975).
25. P. BERNATH AND T. AMANO, in preparation.
26. T. AMANO, P. BERNATH, C. YAMADA, Y. ENDO, AND E. HIROTA, in preparation.
27. M. WONG, T. AMANO, AND P. BERNATH, in preparation.
28. M. WONG, T. AMANO, AND P. BERNATH, *J. Chem. Phys.*, in press.